Chinese Journal of
POLYMER SCIENCE

RESEARCH ARTICLE

https://doi.org/10.1007/s10118-023-3027-y
Chinese J. Polym. Sci. **2024**, *42*, 213–222

Significantly Enhanced Melt Memory Effect of Metallocene-made Isotactic Polypropylene Containing Talc

Hong-Wen Sun[a], Fu-Shan Wang[b], Yan Gao[b], Fu-Qing Wei[c], and Jia-Chun Feng[a*]

[a] *State Key Laboratory of Molecular Engineering of Polymers, Department of Macromolecular Science, Fudan University, Shanghai 200433, China*
[b] *Lanzhou Petrochemical Corporation of PetroChina, Lanzhou 730060, China*
[c] *Lanzhou Petrochemical Research Center, Petrochemical Research Institute of PetroChina, Lanzhou 730060, China*

Electronic Supplementary Information

Abstract The melt memory effect is a widely observed phenomenon in semi-crystalline polymers. In practical applications, various additives are usually introduced into polymers, which may affect their melt memory behavior. In this work, the effect of talc on the melt memory effect of metallocene-made isotactic polypropylene (M-PP) was investigated in detail by using the differential scanning calorimetry. The results indicated that the introduction of talc significantly strengthened the melt memory effect of M-PP. Specifically, the upper limit temperature of *Domain II* increased from 161 °C to 174 °C, resulting in a substantial widening of the temperature range of *Domain IIa* from 1 °C to 14 °C. Analysis of the crystal orientation of the M-PP containing talc cooled from various T_s suggested that the remarkably enhanced melt memory effect could be ascribed to the stabilization of oriented nuclei facilitated by talc. This stabilizing effect was likely attributable to the prefreezing effect or the sorption interaction between talc and the M-PP chains.

Keywords Metallocene-made isotactic polypropylene; Talc; Melt memory effect; Crystal orientation

Citation: Sun, H. W.; Wang, F. S.; Gao, Y.; Wei, F. Q.; Feng, J. C. Significantly enhanced melt memory effect of metallocene-made isotactic polypropylene containing talc. *Chinese J. Polym. Sci.* **2024**, *42*, 213–222.

INTRODUCTION

The melt memory effect is a common phenomenon for semi-crystalline polymer, which has been extensively investigated due to its marked impact on the crystallization behavior of polymers.[1] It is widely accepted that when the melt temperature (T_s) is low enough to leave some self-nuclei in the melt, the crystallization of the polymer is greatly accelerated and the crystal structure is significantly changed in the subsequent cooling process. The melt memory effect of polymers was commonly investigated by employing the differential scanning calorimetry (DSC)-based thermal procedure developed by Fillon *et al*.[2] They categorized the T_s from high to low into three *Domains*, namely *Domain I* (isotropic melt *Domain*), *II* (self-nucleation *Domain*), and *III* (self-nucleation and annealing *Domain*).[2] The *Domain II* was further classified into two sub-*Domains* by Müller *et al*.: *Domain IIa*, in which only a few amorphous ordered structures remained in the melt, and *Domain IIb*, in which the crystal fragment survived in the melt.[3] Recently, the important advances in melt memory effect have been well reviewed by Müller *et al*.[1]

To date, the melt memory effect of various semi-crystalline polymers including homopolymers and copolymers has been studied extensively and several interpretations have been proposed to describe the origin of melt memory effect. For some nonpolar homopolymers, whose *Domain IIa* was generally small or absent, the melt memory effect was commonly ascribed to the crystalline remnants in the melt.[2] In contrast to these nonpolar homopolymers, for some polar homopolymers or some random copolymers, the transition temperature from *Domain I* to *Domain II* was usually located at temperature well above the end of the melting endotherm or even higher than their equilibrium melting temperature (T_m^0).[3–12] In this case, the crystal fragments hardly survived in the melt, and the origin of melt memory effect was attributed to the residual amorphous ordered structure, such as the segmental orientation,[9] the aggregation of long crystallizable sequences,[6,7,11] the partially disentangled regions[12] and so on. In addition to the molecular structure, the introduction of some additives also had an influence on the melt memory effect of the corresponding semi-crystalline polymer. Colonna *et al*. found that the addition of reduced graphene oxide (RGO) made the original *Domain II* in pure poly(butylene terephthalate) (PBT) disappeared in the composite, which was attributed to the formation of extended chain crystals on RGO.[13] Vega *et al*.[14] and Maiz *et al*.[15] also reported the absence of *Domain II* in high density polyethylene containing carbon nanotubes and thermoplastic polyurethane containing nucleating agents due to the supernucleation effect of

* Corresponding author, E-mail: jcfeng@fudan.edu.cn
Received May 21, 2023; Accepted July 13, 2023; Published online August 23, 2023

these additives for the corresponding matrix. Men *et al*. reported a strong melt memory effect in a commercial isotactic polybutene-1 (*i*PB-1) even at temperatures much higher than its T_m^0.[16] They proposed that this unique melt memory effect was associated with the unidentified additives, which stabilized the *i*PB-1 crystals at rather high T_s due to the occurrence of prefreezing.[16] In some of our previous works, it was found that the introduction of nucleation agents calcium pimelate, *N*,*N*′-dicyclohexylterephthalamide, 1,3:2,4-bis(3,4-dimethylbenzylidene)sorbitol and talc, acid scavenger hydrotalcite, as well as lubricant *N*,*N*′-ethylenebis-(stearamide), varied the critical transition temperatures of *Domain I* to *Domain II* or *Domain II* to *Domain III* for isotactic polypropylene (*i*PP) prepared by Ziegler-Natta catalyst and the specific effects differed depending on the additive used.[17–19] These studies fully demonstrated that the addition of some additives influenced the melt memory behavior of polymers. Considering that, on the one hand, the melt memory effect plays a prominent influence on accelerating the crystallization and changing the crystalline structure for semi-crystalline polymer, and on the other hand, in practical application, the introduction of some additives is now the necessary and widely used approach to improve the processability of polymers, optimize the physical properties or endow products with special functions, the investigation of melt memory effect for samples containing additives makes sense from the perspective of both academia and industry.

As a widely used semi-crystalline polymer, *i*PP is often chosen as candidate for research on melt memory effect.[2,4,20–22] The *i*PP prepared by metallocene catalyst (M-PP) attracted much attention due to its more defined microstructures comparing with that of the *i*PP prepared by Ziegler-Natta catalyst (ZN-PP).[23,24] The previous studies revealed that the defects in M-PP chains possessed random distribution due to the single-site of metallocene catalyst on inducing the polymerization of propylene, which was significantly different from that of the ZN-PP who exhibited microstructure with a clustered defects distribution due to the multiple-site of Ziegler-Natta catalyst.[23,24] Recently, we compared the melt memory effects of M-PP and ZN-PP with the similar content of the defect. It was found that when the crystal was fully melted, the melt memory effect still remained for M-PP and disappeared for ZN-PP.[20] Obviously, this different melt memory behaviors for M-PP and ZN-PP were related to their discrepancy in microstructure. The random defects distribution for M-PP resulted in the separation of crystallizable and atactic sequences after the fully melting of the crystals, which lead to the appearance of *Domain IIa* for M-PP, while the clustered defects distribution for ZN-PP was not capable to induce the occurrence of sequence separation and thus the melt memory effect disappeared when the crystal was completely melted.[20] Up to now, the melt memory effect of *i*PP has been extensively studied in both M-PP and ZN-PP,[2,4,20–22] while with regarding to the melt memory effect of *i*PP containing additives, comparing with a few works as aforementioned devoted to investigating the influence of the commonly used additives on the melt memory behavior of ZN-PP,[17–19] as far as we known, no investigation on the effect of additives on that of M-PP has been reported in the previous work. Considering that the melt memory effect of M-PP is obviously distinguished from that of the ZN-PP and the additive addition is also necessary in M-PP, exploring the melt memory behavior of M-PP containing additives is of great scientific and application value.

In this work, talc, a widely used nucleating agent or filler in *i*PP resin, was introduced in M-PP and the melt memory effect of talc-filled M-PP was systematically studied by DSC. It was found that the M-PP containing talc exhibited much wider *Domain II* than that of pure M-PP. By analyzing the melting behavior of these two samples and the crystal structure of samples obtained by cooling from different T_s, the possible reason for talc enhancing the melt memory effect of M-PP was proposed.

EXPERIMENTAL

Materials and Sample Preparation

M-PP employed was a raw powder kindly supplied by Dushanzi Petrochemical Co., (Dushanzi, China). The M_w of this M-PP was 173 kg/mol and the dispersity index was 2.9. The talc employed was a commercial product and its morphology has been characterized in our previous study.[18]

The M-PP was melted mix with 0.1 wt% talc at 180 °C by HAAKE Polylab OS mixer (ThermoFisher, Massachusetts) for 8 min with rotate speed of 80 r/min. 0.1 wt% Irganox 1010 was also introduced into the mixture to avoid the possible thermal degradation of M-PP. Then, the blend was compression-molded into a 0.5 mm sheet under 10 MPa for 5 min at 180 °C. As the reference sample, neat M-PP was also processed in the same way. The sheets of neat M-PP and M-PP containing 0.1 wt% talc was denoted as M-PP/0T and M-PP/0.1T, respectively.

The compression-molded sheets were thermal-treated by a DSC 3+ differential scanning calorimetry (DSC, Mettler Toledo Instruments Inc., Switzerland). The corresponding thermal protocol was as follows: after eliminating thermal history at 200 °C for 5 min, the sheet was cooled to 40 °C to construct "standard" crystallized sample; then, it was heated to the preset T_s, holding for 5 min and finally cooled to 40 °C. The heating/cooling rate in the thermal protocol was set as 10 °C/min.

Characterizations

The crystallization and melting behaviors of M-PP/0T and M-PP/0.1T were characterized by DSC with a rate of 10 °C/min. After the elimination of thermal history at 200 °C, the samples were firstly cooled to 40 °C, then heated to 200 °C and the cooling/heating curves during this process were recorded.

The melt memory effect of M-PP/0T and M-PP/0.1T was also investigated by DSC with a rate of 10 °C/min. The samples in "standard" status were firstly prepared by erasing its thermal history at 200 °C for 5 min and cooling to 40 °C. Then, the "standard" crystallized samples were heated to the preset T_s and hold for 5 min. Finally, the samples were cooled to 40 °C and reheated to 200 °C, where the cooling and reheating curves were recorded to analyze the melt memory effect of samples.

The crystal structure of sample was detected by wide-angle X-ray scattering (WAXS), which was conducted on a Xeuss 2.0 apparatus (Xenocs, Sassenage, France). The incident beam

https://doi.org/10.1007/s10118-023-3027-y

was parallel to the normal direction of the thermal-treated sample.

The crystal structure evolution of "standard" crystallized samples with temperature was investigated by WAXS equipped with a hot stage. The samples in "standard" status were heated from 40 °C to 190 °C at 10 °C/min and the WAXS patterns were recorded at intervals of 2.8 °C.

RESULTS AND DISCUSSION

The Influence of Talc on the Melt Memory Effect of M-PP

The preparation of samples with "standard" status is the prerequisite for studying the melt memory effect. Therefore, the "standard" crystallization and the subsequent melting behaviors of M-PP/0T and M-PP/0.1T were firstly investigated. Fig. 1 displays the corresponding cooling and subsequent heating curves of these two "standard" crystallized samples. As shown in Fig. 1(a), on the cooling curves, the crystallization peak temperatures (T_cs) for M-PP/0T and M-PP/0.1T are 109.5 and 113.7 °C, respectively. The increased T_c for M-PP/0.1T indicated that the introduced talc promoted the crystallization of M-PP. As shown in Fig. 1(b), on the melting curves, there is a similar distinctive melting peak at around 153 °C for M-PP/0T and M-PP/0.1T with the end point of the melting endotherm ($T_{m,end}$) at about 160 °C. That is, the introduction of talc has a negligible effect on the melting behavior of M-PP in "standard" status.

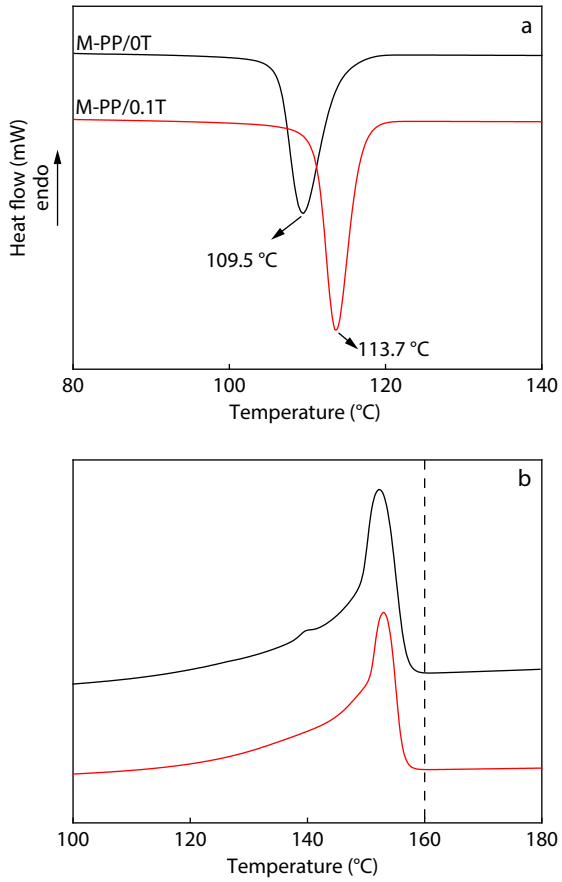

Fig. 1 The DSC (a) cooling curves, (b) melting curves for "standard" crystallized M-PP/0T and M-PP/0.1T.

The crystal structure of "standard" crystallized M-PP/0T and M-PP/0.1T was further characterized by WAXS from surface direction. As shown in Fig. 2, there are six typical peaks at 2θ=14.1°, 16.8°, 18.5°, 20.0°, 21.2° and 21.8° on the WAXS patterns of both samples, where the peak at 2θ of 18.5° attributed to the characteristic peak for the $(130)_\alpha$ plane of α-PP, the peak at 2θ of 20.0° corresponds to the characteristic peak for the $(117)_\gamma$ plane of γ-PP, and the peaks at 2θ of 14.1°, 16.8°, 21.2° and 21.8° were ascribed to the overlapping of the peaks for $(110)_\alpha/(111)_\gamma$, $(040)_\alpha/(008)_\gamma$, $(111)_\alpha/(202)_\gamma$ and $(-131)_\alpha/(041)_\alpha/(026)_\gamma$, respectively. The appearance of these various scattering peaks indicated that α and γ crystals coexisted in the "standard" crystallized samples of M-PP/0T and M-PP/0.1T. According to the literature, the random distribution of defects in M-PP resulted in relatively short isotactic sequences, which was conducive to the generation of γ crystals.[25] By means of the method proposed by Turner-Jones *et al.*,[26] the relative amount of γ form crystals $f(\gamma)$ in M-PP/0T and M-PP/0.1T were calculated to be 39% and 50%, respectively. That is, the introduction of talc increased the relative content of γ crystals in M-PP. This phenomenon was ascribed to the increased crystallization temperature of M-PP with the assistance of talc, which was favorable to the formation of γ-crystals.[27]

In addition to the increased $f(\gamma)$, the intensity of the peak at 2θ=16.8° also obviously reduced for M-PP/0.1T, when comparing with that of M-PP/0T. This reduced intensity of the peak at 2θ=16.8° was commonly reported in talc-filled *i*PP samples, which was caused by the formation of oriented PP crystals induced by the in-plane oriented talc in the matrix.[28,29] The WAXS patterns of M-PP/0T and M-PP/0.1T obtained by observing from the direction of surface and cross section (Fig. S1 in the electronic supplementary information, ESI) further demonstrated that the crystals in M-PP/0T was isotropic and the in-plane oriented talc promoted the generation of oriented α and γ crystals in M-PP/0.1T, where the *b*-axis of the α crystal and the *c*-axis of the γ crystal were parallel to the normal direction of the samples. According to the results of Fig. S1 (in ESI), the $(040)_\alpha$ plane and the $(008)_\gamma$ plane of these oriented α and γ crystals were perpendicular to the incident beam when observing from the surface direction and thus could not be detected, which resulted in the re-

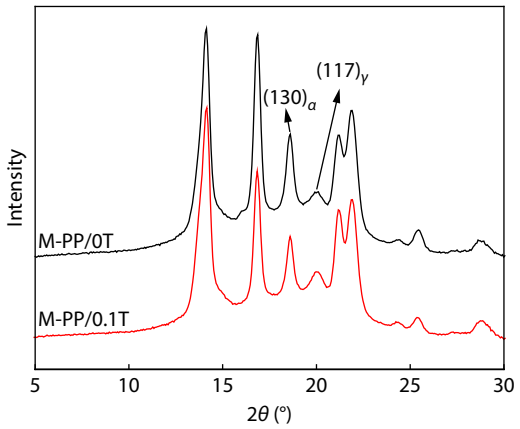

Fig. 2 The 1D-WAXS patterns for "standard" crystallized M-PP/0T and M-PP/0.1T.

https://doi.org/10.1007/s10118-023-3027-y

duced intensity of (040)α/(008)γ plane located at 2θ=16.8°.

After elucidating the effect of talc on the crystallization behavior of M-PP, the DSC-based thermal protocol developed by Fillon *et al.*[2] was employed to investigate the melt memory effect of M-PP/0T and M-PP/0.1T. The T_ss were categorized into three *Domains*, namely *Domain I*, *II*, *III* based on the subsequent thermal behavior of polymers after melting at different T_s.[2] In D*omain I*, where the T_s was sufficiently high to destroy all thermal sensitive nuclei and construct a homogenous melt, the T_c of polymer was independent of T_s; In *Domain II*, where the T_s was low enough to leave some thermal sensitive nuclei in the melt but without occurrence of annealing, the T_c increased as T_s decreased; In *Domain III*, where only partial melting of polymer took place and the un-molten crystals was annealed, the T_c further increased as T_s decreased and a new annealing peak appeared in the high temperature position of the subsequent melting exotherm.[2]

Fig. 3 displays the crystallization curves of samples cooling from different T_s (ranging from 176 °C to 155 °C) and the subsequent melting curves after cooling from different T_s. For M-PP/0T, as the T_s higher than 161 °C, the T_c remained constant at 109.5 °C and was consistent with that of the "standard" crystalized sample (cooling from 200 °C), which indicated that the melt was isotropic and these T_ss were located in *Domain I* (red curves). When the T_s decreased from 161 °C to 156 °C, the T_c gradually increased from 109.6 °C to 123.3 °C and no additional annealing peak appeared on the subsequent melting curves. These increased T_c implied that some self-nuclei survived in the melt and increased in amount with deceased T_s. It was concluded that the T_s located between 161 and 156 °C was in *Domain II* (blue curves). As the T_s decreased to 155 °C, the T_c further increased to 126.8 °C. Notably, an additional annealing peak arose on the corresponding melting curve, which implied that this T_s was located in *Domain III* (green curves). The melt memory effect of M-PP/0.1T was also analyzed on the basis of the same criteria as M-PP/0T. As shown in Figs. 3(c) and 3(d), when the T_s is higher than 175 °C, the T_c is at 113.7 °C, which was independent of T_s and coincident with the "standard" crystallized M-PP/0.1T. These constant T_c indicated that the aforementioned T_s was located in *Domain I*

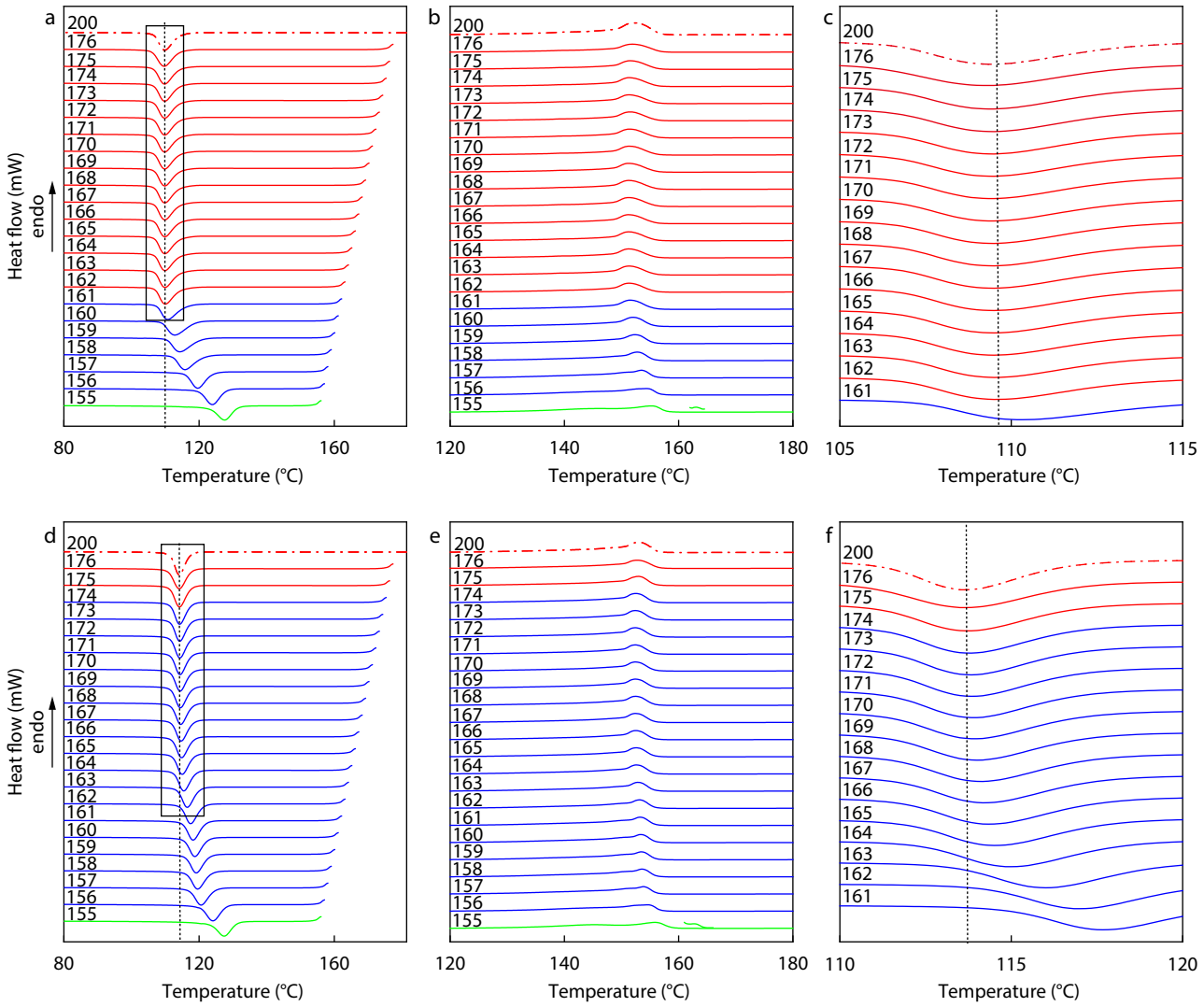

Fig. 3 The DSC (a, d) cooling curves at preset temperature and subsequently (b, e) melting curves for (a, b) M-PP/0T and (d, e) M-PP/0.1T. (c, f) The enlarged view of black rectangle in (a, d).

https://doi.org/10.1007/s10118-023-3027-y

(red curves). When the T_s decreased from 174 °C to 156 °C, the T_c gradually increased from 113.8 °C to 123.5 °C. This increased T_c manifested that some self-nuclei survived in the melt and their amount increased with decreased T_s. Since there was no annealing peak appeared on the high temperature region of the subsequent endotherm, the aforementioned T_s should be located in *Domain II* (blue curves). When the T_s decreased to 155 °C, the T_c further increased to 126.8 °C and a new annealing peak emerged on the subsequent melting curve, which demonstrated that this T_s was located in *Domain III* (green curves).

Based on the above-mentioned results, it was confirmed that the self-nucleation behavior of M-PP/0.1T was obviously different from that of M-PP/0T. To further explore the influence of talc addition on the memory effect of M-PP, the variation of T_c with T_s was superimposed on the "standard" endotherm of the sample and the corresponding three *Domains* for M-PP/0T and M-PP/0.1T were marked. As shown in Fig. 4, the boundary T_s between *Domain II* and *III* (referring to the lowest T_s of *Domain II*) for M-PP/0T and M-PP/0.1T both located at 156 °C, while the transition T_s between *Domain I* and *II* (referring to the lowest T_s of *Domain I*) for M-PP/0.1T was much higher than that of M-PP/0T, which located at 175 and 162 °C, respectively. It was found that the introduction of talc improved the upper limit temperature of *Domain II* and thus largely widened the temperature width of *Domain II* from 6 °C to 19 °C. Notably, the upper limit temperature of *Domain II* for M-PP/0.1T was much higher than its $T_{m,end}$ at 160 °C (marked by the black dotted line). According to Müller *et al.*, *Domain II* could be divided into two sub-*Domains*, *i.e.*, *Domain IIa* and *IIb* by taking $T_{m,end}$ as the boundary.[3] When the T_s in *Domain II* was lower than 160 °C, some crystal fragments survived in the melt and these T_ss were assigned to *Domain IIb*; while when the T_s in *Domain II* was higher than 160 °C, no indication for crystal residue was detected and these T_ss were assigned to *Domain IIa*. The *Domain IIb* of M-PP/0.1T was consistent with that of M-PP/0T. In sharp contrast, the *Domain IIa* of M-PP/0.1T was obviously different from that of M-PP/0T, where the extremely narrow *Domain IIa* with the temperature width of only 1 °C was widened to 14 °C with the introduction of talc. Recall to our previous work, for ZN-PP, additives including talc were reported to widen or shorten the temperature range of *Domain II* by no more than 4 °C.[17–19] Different from ZN-PP in which the additives only slightly influence its melt memory behavior, these above results demonstrated that talc addition significantly strengthened the melt memory effect of M-PP.

The Possible Explanation for the Strengthened Melt Memory Effect of M-PP Containing Talc

Aforementioned DSC results suggested that the introduction of talc remarkably enhanced the melt memory behavior of M-PP. In our previous work, talc was proposed to slightly strengthened melt memory effect of ZN-PP, which was ascribed to the improved thermal stability of *i*PP crystals induced by talc.[18] In this case, the origin of the melt memory effect for talc-filled ZN-PP was attributed to the crystalline remnants in the melt.[18] However, in the present investigation, the upper limit temperature of *Domain IIa* for M-PP/0.1T was much higher than its $T_{m,end}$, which implied that the crystal residues were unlikely to be responsible for the extremely wide *Domain IIa* for M-PP/0.1T. To further rule out the role of the crystal residues on the melt memory effect of M-PP/0.1T, the WAXS was employed to monitor the structure evolution of the "standard" crystallized M-PP/0T and M-PP/0.1T upon heating from 40 °C to 190 °C. As shown in Fig. 5, the typical scattering peaks for M-PP/0T and M-PP/0.1T are only slightly varied when the temperature is lower than 140 °C; further increasing the temperature, the intensities of these peaks continuously reduced and disappeared completely at 164.6 °C. This phenomenon indicated that the bulk melting behavior of M-PP/0.1T was similar with that of the M-PP/0T and there was no obvious difference in thermal stability of the *i*PP crystals for M-PP/0.1T and M-PP/0T. Therefore, the enhanced melt memory effect of M-PP/0.1T should not be ascribed to the crystalline remnants derived from the bulk crystallization.

The early researches showed that the crystals induced by the self-nuclei survived in the melt inherited the orientation of its original status.[30] Our prior work also demonstrated that in talc-filled ZN-PP samples, the nuclei stabilized by talc exhibited specific orientation, which induced the formation of the oriented *i*PP crystals and thus improved the crystal orientation of the sample.[12,18] Conversely, the nuclei unaffected by talc was isotropic, which enabled the generation of

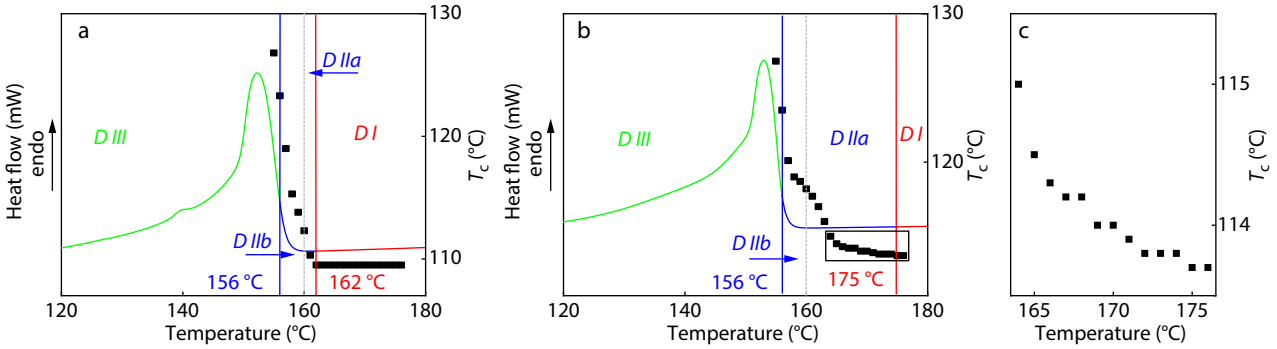

Fig. 4 Three *Domains* for (a) M-PP/0T and (b) M-PP/0.1T superimposed on the "standard" melting curve of the corresponding sample (*Domain I*, *II* and *III* were identified in red, blue and green, respectively). The red and blue solid line represented the transition temperatures of *Domain I* to *II* and *Domain II* to *III*, which were the lowest T_s for *Domain I* and *Domain II*, respectively. The black dotted line represented the end melting temperature of the sample, which divided the *Domain II* into two sub-*Domains*: *Domain IIa* and *Domain IIb*. The squares represented the variation of T_c with T_s. (c) The enlarged view of the variation of T_c with T_s in the range of 164–176 °C.

https://doi.org/10.1007/s10118-023-3027-y

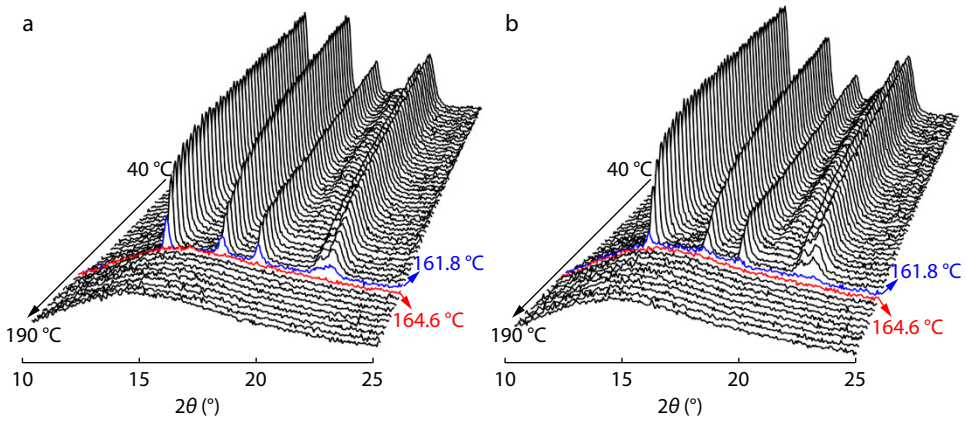

Fig. 5 WAXS patterns of "standard" crystallized (a) M-PP/0T and (b) M-PP/0.1T upon heating.

isotropic *i*PP crystals and thus decreased the crystal orientation of the sample.[18] That is, the properties of the nuclei survived in the melt at different T_s played a crucial role in determining the ultimate crystal orientation of the products.[18] Building upon these studies, it was proposed that the nature of the residual nuclei in the melt can be inferred in reverse and on the basis of this, the remarkable effect of talc on enhancing the melt memory effect of M-PP can be explained.

WAXS was employed to characterize the crystal orientation of M-PP/0T and M-PP/0.1T cooled from various T_s (ranging from 156 °C to 176 °C) by observing from surface direction of the samples. As shown in Fig. 6, although similar six typical peaks arising from the *α* and *γ* crystals can be detected on the WAXS patterns of M-PP/0T and M-PP/0.1T cooled from different T_s, some obvious differences was not negligible for these samples. Notably, the intensity of the peak at 2θ=16.8° was reduced for M-PP/0.1T when comparing with that of M-PP/0T cooled from same T_s. This reduced intensity was caused by the formation of oriented *i*PP crystals induced by in-plane oriented talc in M-PP/0.1T. Besides, it was worth noting that the intensity of the peak at 2θ=16.8° for M-PP/0.1T varied regularly with the change of T_s, *i.e.*, it remained stable at higher T_s, decreased obviously at medium T_s, and increased significantly at lower T_s. These results indicated that the crystal orientation of M-PP/0.1T showed regular changes with T_s.

The intensity ratio of the peak at 2θ of 16.8° and 14.1° ($I_{16.8°}/I_{14.1°}$) was commonly utilized to estimate the crystal orientation of *i*PP samples.[28,31] This ratio was reported to be located between 0.67–0.77 for samples only containing isotropic *α* crystals.[28,31] Meanwhile, the $I_{16.8°}/I_{14.1°}$ value decreased for samples possessing oriented *α* crystals induced by in-plane oriented talc, since the existence of these oriented *α* crystals reduced the intensity of the peak at the 2θ of 16.8°.[28,31] It was generally accepted that the higher the content of talc-induced oriented *α* crystals in *i*PP samples, the lower this ratio was.[28,31] In our work, the introduction of in-plane oriented talc not only induced the formation of oriented *α* crystals but also enabled the generation of oriented *γ*

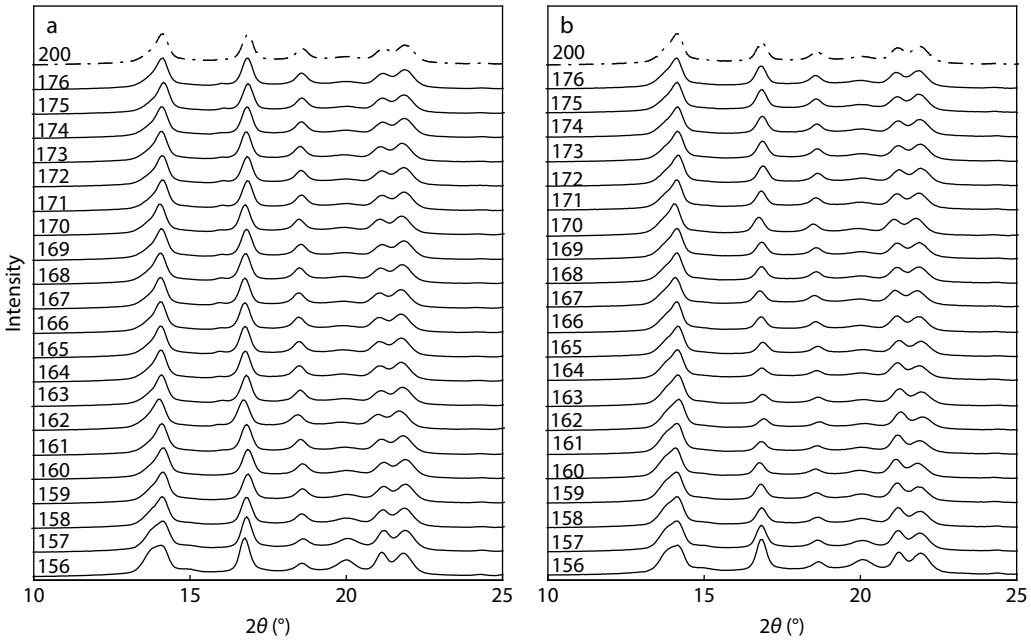

Fig. 6 WAXS patterns of (a) M-PP/0T and (b) M-PP/0.1T cooled from various T_ss.

https://doi.org/10.1007/s10118-023-3027-y

crystals in M-PP. In view of the results of Fig. S1 (in ESI), the existence of these oriented γ crystals also decreased the intensity of the peak at the 2θ of 16.8° and thus reduced the $I_{16.8°}/I_{14.1°}$ value. Therefore, when the oriented α and γ crystals coexisted in M-PP, the $I_{16.8°}/I_{14.1°}$ value can also utilized to estimate its crystal orientation. The lower the ratio, the higher the content of oriented α and γ crystals in M-PP.

Before investigating the influence of T_s on the crystal orientation of M-PP/0T and M-PP/0.1T by analyzing the $I_{16.8°}/I_{14.1°}$ values of various samples, the crystal orientation of the "standard" crystallized M-PP/0T and M-PP/0.1T (the samples cooled from 200 °C) were firstly evaluated, whose $I_{16.8°}/I_{14.1°}$ values were 0.90 and 0.63, respectively. The lower $I_{16.8°}/I_{14.1°}$ value for M-PP/0.1T should be caused by the presence of talc-induced oriented α and γ crystals. It is worth noting that although this value for "standard" crystallized M-PP/0T, *i.e.*, 0.90, was not within the range of 0.67–0.77, it did not imply the presence of oriented crystals in this sample, as the criterion for proving the formation of isotropic PP crystals with the $I_{16.8°}/I_{14.1°}$ value in the range of 0.67–0.77 was only applied to α crystals, which was not appropriate for the "standard" crystallized M-PP/0T, where α and γ crystals coexisted. In fact, the WAXS patterns displayed in Fig. S1 (in ESI) already demonstrated that the α and γ crystals in "standard" crystallized M-PP/0T were isotropic. That is, when the α and γ crystals coexisted in the sample, the $I_{16.8°}/I_{14.1°}$ value for isotropic PP crystals was enhanced. Based on this result, it was speculated that the $I_{16.8°}/I_{14.1°}$ value for isotropic γ crystal was higher than that of the isotropic α crystal, which resulted in the higher $I_{16.8°}/I_{14.1°}$ value for the isotropic *i*PP crystals in "standard" crystallized M-PP/0T.

To comprehensively evaluate the crystal orientation of M-PP/0T and M-PP/0.1T cooled from different T_s ranging from 156 °C to 176 °C, the $I_{16.8°}/I_{14.1°}$ values of these samples were calculated and outlined in Fig. 7 (specific values of these samples are summarized in Table S1 in ESI). The $I_{16.8°}/I_{14.1°}$ values for M-PP/0T cooled from different T_s within the range of 158–176 °C were predominantly hovered around 0.90, which was similar with that of the "standard" crystallized M-PP/0T, indicating the generation of isotropic *i*PP crystals in these samples. This phenomenon was consistent with our previous work, which proposed that the crystals in neat *i*PP samples cooled from different T_s were all isotropic, since the isotropic nuclei survived in the melt only enabled the generation of isotropic crystals.[18] Notably, further decreased the T_s to 157 and 158 °C, the $I_{16.8°}/I_{14.1°}$ values noticeably increased to 1.0 and 1.2, respectively. The increased $I_{16.8°}/I_{14.1°}$ values for these two samples did not indicate the formation of oriented crystals in the samples but might be caused by the increased content of γ crystals in these two samples (the $f(\gamma)$ of various samples were shown in Table S1 in ESI).

For M-PP/0.1T, as shown in Fig. 7, it has significantly reduced $I_{16.8°}/I_{14.1°}$ values comparing with that of M-PP/0T when cooled from the same T_s. More specifically, the values of M-PP/0.1T slightly fluctuated at around 0.63 (similar with that of the "standard" crystallized M-PP/0.1T) as the T_s≥175 °C, obviously reduced from 0.57 to 0.28 when the T_s decreased from 174 °C to 162 °C, and obviously increased from 0.32 to 1.13 as the T_s decreased from 161 °C to 156 °C. Combining the result of melt memory effect for M-PP/0.1T shown in Fig. 4(b), it was

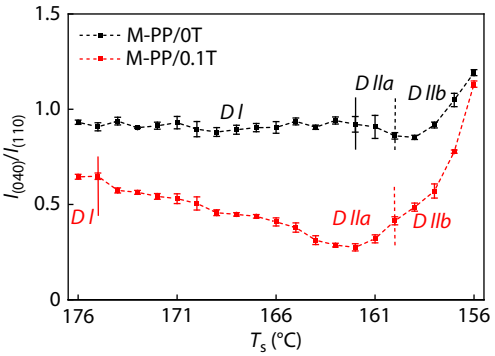

Fig. 7 The $I_{(040)}/I_{(110)}$ values of M-PP/0T and M-PP/0.1T cooled from various T_s.

concluded that when the T_s fell within *Domain I*, the crystal orientation of M-PP/0.1T was irrelevant with T_s, which was in accordance with our previous work;[18] when the T_s lined in *Domain II*, the crystal orientation of M-PP/0.1T noticeably increased with decreased T_s at the higher temperature part of *Domain II* (162–174 °C, assigned to *Domain IIa*) and remarkably decreased with decreased T_s at the lower temperature part of *Domain II* (156–161 °C). Moreover, the orientational order parameters of the $(040)_\alpha/(008)_\gamma$ reflection for M-PP/0.1T cooled from various T_ss (Figs. S2 and S3 in ESI) also demonstrated that the crystal orientation of M-PP/0.1T firstly increased and then decreased with the decreased T_s when the T_s located in *Domain II*. The variation of crystal orientation with T_s in *Domain II* for M-PP/0.1T provided insights into the nature of these residual nuclei in the melt. At the higher temperature part of *Domain II*, the increased crystal orientation of M-PP/0.1T with decreased T_s manifested that some oriented nuclei stabilized by talc survived in the melt and their quantity continually increased with decreased T_s, while at the lower temperature part of *Domain II*, the decreased crystal orientation of M-PP/0.1T with decreased T_s. This implied that in addition to these oriented nuclei, some isotropic nuclei unaffected by talc also remained in the melt and their quantity continually increased with decreased T_s as well. Based on the aforementioned analysis, it was unquestionable that the significantly enhanced melt memory effect for M-PP/0.1T in contrasted to M-PP/0T must be related to these oriented nuclei stabilized by talc, which remained stable even well above the bulk melting temperature of M-PP.

The origin of these talc-stabilized oriented nuclei with exceptional thermal stability may be correlated with the possible existing prefeezing effect[32–35] between the M-PP and talc. This prefreezing effect proposed by Thurn-Albrecht *et al*. suggested that the occurrence of prefreezing between the matrix and substrate enabled the generation of thermodynamically stable crystals on the surface of the substrate, which kept stable well above the bulk melting temperature of the matrix.[32–35] Recently, Men *et al*. reported that the presence of an unidentified additive in commercial *i*PB-1 significantly strengthened the melt memory effect of *i*PB-1.[16] They attributed this strong melt memory effect to the additive-stabilized *i*PB-1 crystals, which survived at the temperature much higher than its bulk melting temperature due to the occurrence of prefreezing and acted as potential nuclei to accel-

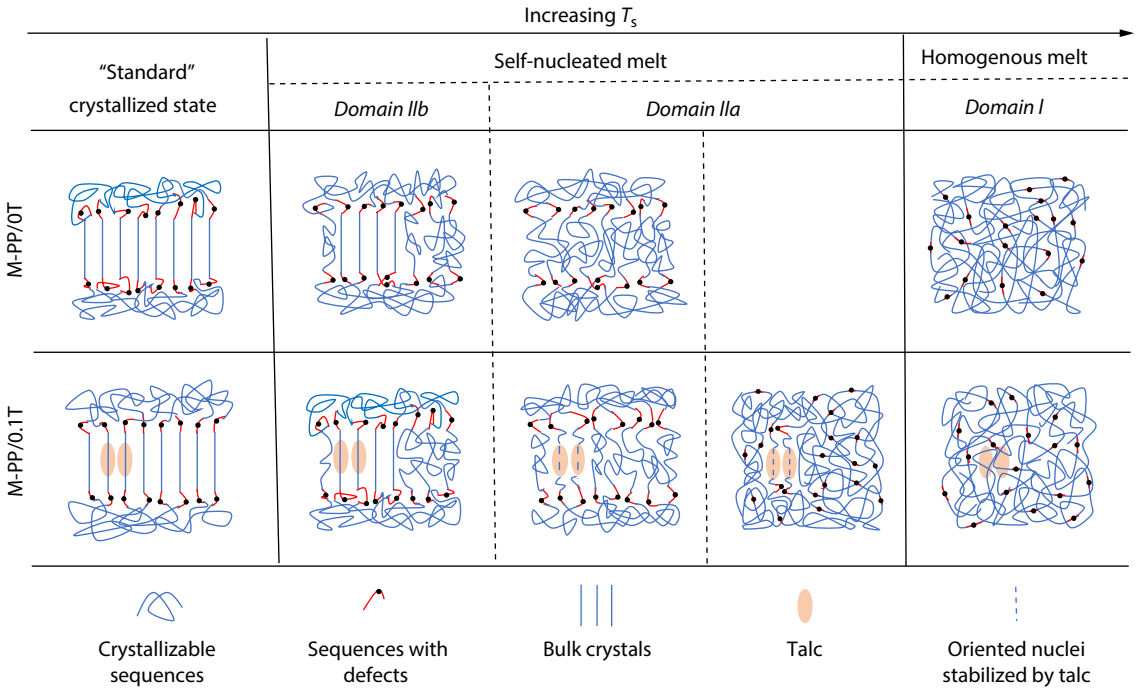

Fig. 8 The possible structure evolution of M-PP/0T and M-PP/0.1T during heating process.

erate the crystallization of *i*PB-1.[16] In our study, considering that the talc-stabilized nuclei also survived in the melt when the T_s was much higher than its bulk melting temperature, this prefreezing effect may also exist between talc and M-PP and thus enhanced the upper limited temperature of Domain II for M-PP/0.1T. Based on the prefreezing theory, the crystals prefrozen on the substrates commonly possessed unique orientation given by the substrate, which served as the ideal nuclei to initiate the bulk crystallization and enabled the generation of oriented crystals.[32–35] The preceding results regarding the crystal orientation of M-PP/0.1T cooled from different T_s indeed demonstrated the existence of the oriented nuclei stabilized by talc, which induced the formation of oriented *i*PP crystals during the crystallization process. This phenomenon indirectly supported the occurrence of prefreezing between talc and M-PP.

In addition to the prefreezing effect, the introduced additives were also reported to be capable of absorbing the polymer chains and thus fixing the residual segmental orientation after the completely melting of the crystals, which was able to induce oriented recrystallization of polymer.[36,37] This possible existing sorption effect between talc and M-PP chains may also responsible for the origin of these talc-stabilized oriented nuclei in the melt. When the crystals on talc was fully melted, some oriented segments might still survive on surface of the talc due to the slow relaxation of the M-PP chains under the sorption action of talc, which remarkably strengthened the melt memory effect of M-PP. Meanwhile, these oriented segments anchored on talc acted as the potential oriented nuclei to induce the formation of oriented *i*PP crystals in subsequent recrystallization process.

On the basis of the preceding discussion, we have proposed the plausible structure evolution of M-PP/0T and M-PP/0.1T upon heating to elucidate the role of talc on enhancing the melt memory effect of M-PP. As shown in Fig. 8, referring to our previous work,[20] for M-PP/0T, when the T_s fell within *Domain IIb*, some crystal fragments with high thermal stability survived in the melt; increasing the T_s to the temperature range of *Domain IIa*, the random defects distribution for M-PP led to the separation of crystallizable and atactic sequences after the fully melting of the crystals; further increasing the T_s to the temperature range of *Domain I*, this sequence separation vanished and resulted in the formation of the homogenous melt without melt memory effect. In clear contrast, for M-PP/0.1T, when the T_s lied in *Domain IIb*, similar to M-PP/0T, some crystalline remnants survived in the melt; increasing the T_s to the lower temperature part of *Domain IIa*, in addition to the sequence separation, some oriented nuclei stabilized by talc (possibly the crystals prefrozen on the talc or the oriented segments absorbed on the surface of talc) also remained in the melt; further increasing the T_s to the higher temperature part of *Domain IIa*, although the sequence separation vanished, these oriented nuclei still survived in the melt, which resulted in the remarkablely enhanced melt memory effect for M-PP/0.1T compared to M-PP/0T; when the T_s lied in *Domain I*, these oriented nuclei vanished as well leading to the disappearance of the melt memory effect for M-PP/0.1T.

CONCLUSIONS

In this work, the effect of talc on the melt memory effect of M-PP was investigated in detail. By comparing the melt memory effect of neat M-PP (M-PP/0T) and M-PP containing 0.1% talc (M-PP/0.1T), it was found that the introduction of talc obviously enhanced the upper limit temperature of *Domain II* from 161 ℃ to 174 ℃ and thus widened the temperature width of *Domain IIa* from 1 ℃ to 14 ℃. The structure evolution of the "standard"

https://doi.org/10.1007/s10118-023-3027-y

crystallized M-PP/0T and M-PP/0.1T upon heating ruled out the role of the bulk crystal residues on enhancing the melt memory effect of M-PP/0.1T. The crystal orientation of M-PP/0.1T cooled from different T_s reflected the properties of residual nuclei at different T_s to a certain extent. The results of WAXS indicated that some oriented nuclei stabilized by talc survived at the temperature well above the bulk melting temperature of M-PP, which obviously enhanced the melt memory effect of M-PP. These oriented nuclei stabilized by talc might originate from prefreezing effect or the sorption interaction between talc and the M-PP chains.

Conflict of Interests

The authors declare no interest conflict.

Electronic Supplementary Information

Electronic supplementary information (ESI) is available free of charge in the online version of this article at http://doi.org/10.1007/s10118-023-3027-y.

ACKNOWLEDGMENTS

This work was financially supported by the National Natural Science Foundation of China (Nos. 51973037 and 52173056) and PetroChina Company Limited, China.

REFERENCES

1 Sangroniz, L.; Cavallo, D.; Müller, A. J. Self-nucleation effects on polymer crystallization. *Macromolecules* **2020**, *53*, 4581–4604.
2 Fillon, B.; Wittmann, J.; Lotz, B.; Thierry, A. Self-nucleation and recrystallization of isotactic polypropylene (*α* phase) investigated by differential scanning calorimetry. *J. Polym. Sci., Part B: Polym. Phys.* **1993**, *31*, 1383–1393.
3 Sangroniz, L.; Alamo, R.; Cavallo, D.; Santamaría, A.; Müller, A.; Alegría, A. Differences between isotropic and self-nucleated PCL melts detected by dielectric experiments. *Macromolecules* **2018**, *51*, 3663–3671.
4 Li, X.; Ma, Z.; Su, F.; Tian, N.; Ji, Y.; Lu, J.; Wang, Z.; Li, L. New understanding on the memory effect of crystallized *i*PP. *Chinese J. Polym. Sci.* **2014**, *32*, 1224–1233.
5 Sangroniz, L.; Cavallo, D.; Santamaria, A.; Müller, A. J.; Alamo, R. G. Thermorheologically complex self-seeded melts of propylene-ethylene copolymers. *Macromolecules* **2017**, *50*, 642–651.
6 Mamun, A.; Chen, X.; Alamo, R. G. Interplay between a strong memory effect of crystallization and liquid-liquid phase separation in melts of broadly distributed ethylene-1-alkene copolymers. *Macromolecules* **2014**, *47*, 7958–7970.
7 Gao, H.; Vadlamudi, M.; Alamo, R. G.; Hu, W. Monte Carlo simulations of strong memory effect of crystallization in random copolymers. *Macromolecules* **2013**, *46*, 6498–6506.
8 Liu, X.; Wang, Y.; Wang, Z.; Cavallo, D.; Müller, A. J.; Zhu, P.; Zhao, Y.; Dong, X.; Wang, D. The origin of memory effects in the crystallization of polyamides: role of hydrogen bonding. *Polymer* **2020**, *188*, 122117.
9 Lorenzo, A. T.; Arnal, M. L.; Sanchez, J. J.; Müller, A. J. Effect of annealing time on the self-nucleation behavior of semicrystalline polymers. *J. Polym. Sci., Part B: Polym. Phys.* **2006**, *44*, 1738–1750.
10 Marxsen, S. F.; Alamo, R. G. Melt-memory of polyethylenes with halogen substitution: random vs. precise placement. *Polymer* **2019**, *168*, 168–177.
11 Reid, B. O.; Vadlamudi, M.; Mamun, A.; Janani, H.; Gao, H.; Hu, W.; Alamo, R. G. Strong memory effect of crystallization above the equilibrium melting point of random copolymers. *Macromolecules* **2013**, *46*, 6485–6497.
12 Luo, C.; Sommer, J. U. Frozen topology: entanglements control nucleation and crystallization in polymers. *Phys. Rev. Lett.* **2014**, *112*, 195702.
13 Colonna, S.; Pérez-Camargo, R. A.; Chen, H.; Liu, G.; Wang, D.; Müller, A. J.; Saracco, G.; Fina, A. Supernucleation and orientation of poly(butylene terephthalate) crystals in nanocomposites containing highly reduced graphene oxide. *Macromolecules* **2017**, *50*, 9380–9393.
14 Vega, J. F.; Da Silva, Y.; Vicente-Alique, E.; Nunez-Ramirez, R.; Trujillo, M.; Arnal, M. L.; Müller, A. J.; Dubois, P.; Martinez-Salazar, J. Influence of chain branching and molecular weight on melt rheology and crystallization of polyethylene/carbon nanotube nanocomposites. *Macromolecules* **2014**, *47*, 5668–5681.
15 Maiz, J.; Fernandez-d'Arlas, B.; Li, X.; Balko, J.; Poeselt, E.; Dabbous, R.; Thurn-Albrecht, T.; Müller, A. J. Effects and limits of highly efficient nucleating agents in thermoplastic polyurethane. *Polymer* **2019**, *180*, 121676.
16 Liu, P.; Xue, Y.; Men, Y. Melt memory effect beyond the equilibrium melting point in commercial isotactic polybutene-1. *Ind. Eng. Chem. Res.* **2019**, *58*, 5472–5478.
17 Yue, Y.; Sha, X.; Wang, F.; Gao, Y.; Zhang, L.; Wang, X.; Feng, J. The effect of *β*-nucleating agent on the self-nucleation of isotactic polypropylene. *Polymer* **2021**, *229*, 124009.
18 Sun, H.; Wang, L.; Yi, J.; Wang, F.; Gao, Y.; Sha, X.; Feng, J. The influence of melt temperature on the crystal orientation of polypropylene containing talc. *Polymer* **2022**, *256*, 125179.
19 Yue, Y.; Sha, X.; Wang, F.; Gao, Y.; Zhang, L.; Zhu, Y.; Wang, X.; Feng, J. Non-negligible effect of additives in the application of successive self-nucleation and annealing fractionation for microstructure characterization of matrix resin in additive-containing samples. *ACS Appl. Polym. Mater.* **2021**, *3*, 4634–4644.
20 Wang, X.; Yi, J.; Wang, L.; Feng, J. Comparison of the melt memory effects in matched fractions segregated from Ziegler-Natta and metallocene-made isotactic polypropylene with similar total defect content. *Polymer* **2021**, *230*, 124060.
21 Zhu, X.; Yan, D.; Yao, H.; Zhu, P. *In situ* FTIR spectroscopic study of the regularity bands and partial-order melts of isotactic poly (propylene). *Macromol. Rapid Commun.* **2000**, *21*, 354–357.
22 Dai, P. S.; Cebe, P.; Capel, M. Thermal analysis and X-ray scattering study of metallocene isotactic polypropylene prepared by partial melting. *J. Polym. Sci., Part B: Polym. Phys.* **2002**, *40*, 1644–1660.
23 De Rosa, C.; Auriemma, F.; Spera, C.; Talarico, G.; Tarallo, O. Comparison between polymorphic behaviors of Ziegler-Natta and metallocene-made isotactic polypropylene: the role of the distribution of defects in the polymer chains. *Macromolecules* **2004**, *37*, 1441–1454.
24 Chang, H.; Zhang, Y.; Ren, S.; Dang, X.; Zhang, L.; Li, H.; Hu, Y. Study on the sequence length distribution of polypropylene by the successive self-nucleation and annealing (SSA) calorimetric technique. *Polym. Chem.* **2012**, *3*, 2909–2919.
25 Auriemma, F.; De Rosa, C. Crystallization of metallocene-made isotactic polypropylene: Disordered modifications intermediate between the *α* and *γ* forms. *Macromolecules* **2002**, *35*, 9057–9068.
26 Jones, A. T.; Aizlewood, J. M.; Beckett, D. Crystalline forms of isotactic polypropylene. *Makromol. Chem.* **1964**, *75*, 134–158.
27 Foresta, T.; Piccarolo, S.; Goldbeck-Wood, G. Competition between α and γ phases in isotactic polypropylene: effects of

ethylene content and nucleating agents at different cooling rates. *Polymer* **2001**, *42*, 1167–1176.
28 Choi, W. J.; Kim, S. C. Effects of talc orientation and non-isothermal crystallization rate on crystal orientation of polypropylene in injection-molded polypropylene/ethylene-propylene rubber/talc blends. *Polymer* **2004**, *45*, 2393–2401.
29 Branciforti, M. C.; Oliveira, C. A.; De Sousa, J. A. Molecular orientation, crystallinity, and flexural modulus correlations in injection molded polypropylene/talc composites. *Polym. Adv. Technol.* **2010**, *21*, 322–330.
30 Xu, J.; Ma, Y.; Hu, W.; Rehahn, M.; Reiter, G. Cloning polymer single crystals through self-seeding. *Nat. Mater.* **2009**, *8*, 348–353.
31 Rybnikář, F. Orientation in composite of polypropylene and talc. *J. Appl. Polym. Sci.* **1989**, *38*, 1479–1490.
32 Flieger, A. K.; Schulz, M.; Thurn-Albrecht, T. Interface-induced crystallization of polycaprolactone on graphite *via* first-order prewetting of the crystalline phase. *Macromolecules* **2017**, *51*, 189–194.
33 Dolynchuk, O.; Tariq, M.; Thurn-Albrecht, T. Phenomenological theory of First-order prefreezing. *J. Phys. Chem. Lett.* **2019**, *10*, 1942–1946.
34 Tariq, M.; Dolynchuk, O.; Thurn-Albrecht, T. Effect of substrate interaction on thermodynamics of prefreezing. *Macromolecules* **2019**, *52*, 9140–9148.
35 Löhmann, A. K.; Henze, T.; Thurn-Albrecht, T. Direct observation of prefreezing at the interface melt-solid in polymer crystallization. *Proc. Natl. Acad. Sci.* **2014**, *111*, 17368–17372.
36 Ma, L.; Zhou, Z.; Zhang, J.; Sun, X.; Li, H.; Zhang, J.; Yan, S. Temperature-dependent recrystallization morphologies of carbon-coated isotactic polypropylene highly oriented thin films. *Macromolecules* **2017**, *50*, 3582–3589.
37 Ma, L.; Zhang, J.; Memon, M. A.; Sun, X.; Li, H.; Yan, S. Melt recrystallization behavior of carbon-coated melt-drawn oriented isotactic polypropylene thin films. *Polym. Chem.* **2015**, *6*, 7524–7532.

https://doi.org/10.1007/s10118-023-3027-y